Eur. Phys. J. B **8**, 225–231 (1999)

THE EUROPEAN PHYSICAL JOURNAL B

EDP Sciences

Formation of ordered micro-porous membranes

O. Pitois[1,a] and B. François[2]

[1] Laboratoire des Matériaux et Structures du Génie Civil[b], CNRS/LCPC, 2 allée Kepler, 77420 Champs-sur-Marne, France
[2] Laboratoire de Recherche sur les Matériaux Polymères, CNRS/UPPA, Centre Hélioparc Pau-Pyrénées, 2 avenue du Président Angot, 64000 Pau, France

Received: 18 August 1998

Abstract. Regular micro-porous polymeric membranes have recently been discovered by rapidly evaporating a solution of CS_2 containing poly(*p*-phenylene)-block-polystyrene [1]. 1,2-dichloroethane (a chlorated solvent in which polystyrene gel phase has never been observed) is also found to produce ordered structures, which definitively excludes eventual effect of the gelation process during the membrane formation. The observation of the solution surface during the solvent evaporation reveals the growing of micron-sized water droplets trapped at the surface and forming compact aggregates. The study of the solution/water interface shows that the water droplets profile is in agreement with the pore shape observed in the membranes. Moreover, the copolymer was found to precipitate at the interface, forming a layer encapsulating the droplets and preventing their coalescence. In that way, the final structure results from the droplets stacking under the action of large surface currents. Finally, we argue that the decisive element in the formation of ordered structures is the ability of the polymer to precipitate at the solution/water interface, which seems to be related the star-polymer microstructure.

PACS. 81.05.Rm Porous materials; granular materials – 68.10.Jy Kinetics (evaporation, adsorption, condensation, catalysis, etc.) – 71.20.Rv Polymers and organic compounds

1 Introduction

Porous materials with a perfect arrangement of pores present interesting properties for technological applications. One of these potential applications is related to the particular optical properties of three-dimensional regular networks of pores with sub-micronic size (photonic crystals). Such structures have recently been prepared from polymer solutions [1]. The resulting microporous membranes are constituted of one or several layers of spherical pores organized in a compact hexagonal network. The pores of the upper layer are open so that the surface of the film is made by an arrangement of circular holes organized in a triangular lattice (see Fig. 1). The preparation method consists in rapidly evaporating a layer of solution spread on a flat support in the presence of moisture (the preparation can be accelerated using a flow of nitrogen containing water vapour). The solution is composed of a volatile solvent (carbon disulphide: CS_2, $T_b = 46\,^{\circ}C$) and a poly(*p*-phenylene)-block-polystyrene (PS-PPP). The use of CS_2 turned out to be essential for preparing well-structured membranes. Besides, several polymers were found to produce regular structures: star-polystyrenes, associative polystyrenes (linear polystyrene chains carrying at one of their ends a polar group able to associate in non-polar solvents [2] such as CS_2) and other rod-coil block copolymers based on polystyrene sequences. One of the particularities of these solutions lies

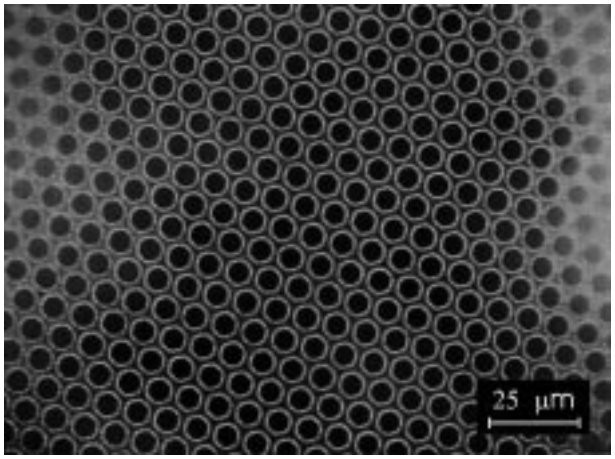

Fig. 1. Optical micrograph showing an example of membrane surface, obtained by rapidly evaporating a polymer solution in the presence of moisture. Solution: PS-PPP block copolymer ($M_w = 30\,000{-}3\,000$) in 1,2-dichloroethane (0.02 g/cm^3).

[a] e-mail: olivier.pitois@lcpc.fr
[b] CNRS-UMR 113

in the star-polymer microstructure. Indeed, CS_2 is a selective solvent for PS so that an aggregation process generally takes place. In particular, PS-PPP forms quasi-spherical micellar aggregates composed of a solid PPP core (30–150 Å) surrounded by a shell of PS sequences [3]. The star-polymer morphology is believed to be a determinant element in the mechanism of formation of the honeycomb structure, all the more because disordered membranes were obtained from usual linear polystyrenes. A second particularity of these solutions is related to the specific ability of PS sequences to form a thermo-reversible gel at ambient temperature in the presence of CS_2. Besides, a recent study of the gelation properties of PS/CS_2 solutions has revealed that this process is more pronounced in the case of star-polystyrenes composed of three and four branches, compared to linear polystyrenes with the same molar mass [4]. While the presence of moisture in the surrounding atmosphere has been proved to be essential for producing ordered membranes, the mechanisms leading to the establishment of the structure still remain unclear; especially with regard to the appearance of the gel phase during the solvent evaporation, which is expected to play a crucial role in the process [5]. This paper presents new interesting results allowing to determine the key processes in the formation of regular polymeric membranes. A qualitative description of the establishment of the structure is given. In Section 2, we present results for gelation temperature measurements. Sections 3 and 4 deal with the wetting properties of the water/solution system and optical microscopy observations. A mechanism of formation is suggested in Section 4, in the light of these new elements.

2 Gelation temperature measurements

Contrary to star-PS and PS-PPP in CS_2 solutions, disordered microstructures were generally obtained with linear PS solutions, so that it seemed interesting to compare the gelation temperatures of these solutions. The ball-drop method [6] was used: gels were prepared by first dissolving the polymer at the desired concentration in CS_2 at room temperature in a tube then sealed and cooled slowly. Afterwards a steel ball was placed on the top of the gel and the temperature was allowed to rise ($\sim 1\,^\circ$C/min). The temperature at which the steel ball began to fall was taken as the gel melting temperature. Gelation/melting temperatures are presented in Figure 2 as a function of the polymer concentration for PS-PPP (molar mass $M_w = 30\,000{-}3\,000$) and star-PS (70 branches $\times\, 6\,000$). The temperatures for atactic linear PS (of molar mass approximately equal to that of star-PS) have been plotted for comparison (result extracted from Ref. [9]). These results show that the gelation process is less pronounced for star-polystyrene than for the linear PS. In the same way, gelation temperatures for PS-PPP/CS_2 solutions were found to be lower as expected, considering the molecular aggregates formed in the solution. As the temperature of the solution is close to 0 °C during the process of formation of membranes, it can be deduced from Figure 2 that the polymer concentrations at the sol/gel transition (for the three tested polymers) are not significantly different at this temperature. For that reason, it seems hardly likely that the gelation process contribute to the formation of ordered structures in the case of star-PS and PS-PPP polymers.

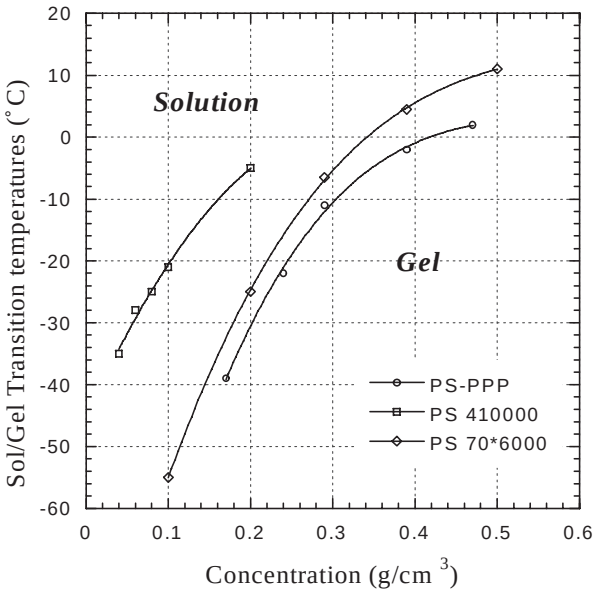

Fig. 2. Sol-gel transition temperatures obtained with carbon disulphide solutions containing a PS-PPP block copolymer ($M_w = 30\,000{-}3\,000$), a star-polystyrene ($M_w = 70 \times 6\,000$) and a linear PS ($M_w = 410\,000$) from reference [9].

3 Wetting properties

As the formation of the structure is induced by condensation of water vapour on the solution surface, we have been interested in the interface properties of the system composed of water and PS-PPP/CS_2 solution.

3.1 Droplet shape

We have been first interested in the shape of a water lens floating at the surface of CS_2 solutions (pure solvent and PS-PPP solution). A water drop (volume $\sim 5\,\mu$l) was placed on the surface of the solution contained in a cubic glass cell (side = 30 mm). The solution was cooled and the observation cell was closed in order to limit the solvent evaporation. An optical device allowed to photograph the drop floating on the solution, as shown in Figure 3: the drop is nearly spherical and is situated below the solution surface for the most part (the top of the water drop is hidden by the meniscus formed by the solution on the cell wall). Considering now a micron-sized droplet, the influence of gravity forces on the droplet shape can be neglected and the water lens is then composed of two spherical segments whose radii are completely determined

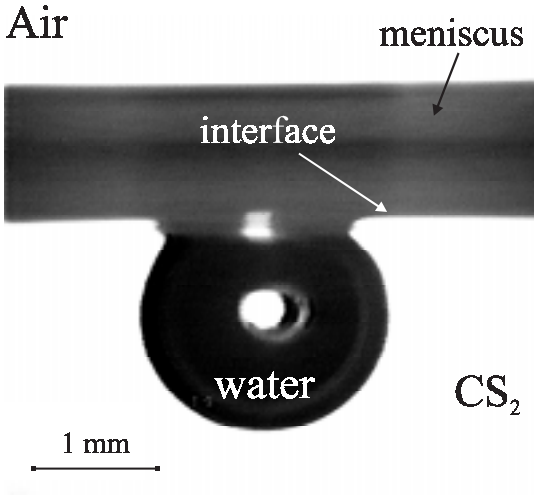

Fig. 3. Photograph of a water drop floating at the CS_2 surface.

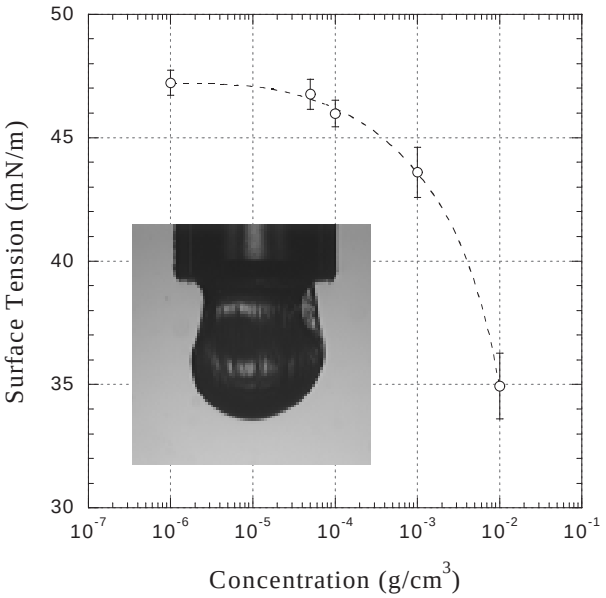

Fig. 4. Interface water/(CS_2 + PS-PPP): Results from surface tension meaurements using the pendant drop method (see Ref. [8]). The visualization of the pendant drop reveals the presence of a solid layer at the interface between the two liquids. This layer can be made clearly visible by partially sucking up the solution contained in the drop (see picture).

by surface tension forces. Contact angles can be calculated from the following expression [7]:

$$\cos\theta_{ij} = \frac{1 + (\gamma_{ij}/\gamma_{jk})^2 - (\gamma_{ik}/\gamma_{jk})^2}{2(\gamma_{ij}/\gamma_{jk})} \qquad (1)$$

where γ_{ij} is the surface tension between i and j phases, and θ_{ij} is the angle formed by interface (ij) at the three phases contact line. The shape of the droplet in Figure 3 is compatible with electron scanning microscopy observations of ordered membranes [1], showing micron-sized spherical cells. We can therefore reasonably suppose that the membranes cells are formed by the condensation of water vapour in the shape micron-sized droplets whose profile is determined by expression (1).

3.2 Surface tension

The pendant drop method [8] has been used to measure the surface tension between water and solutions of PS-PPP/CS_2 (in a concentration range 10^{-6}–10^{-2} g/cm^3). A drop of solution (the heavier phase) was formed in water by means of a syringe. An image of the resulting hanging drop was acquired using a CCD camera and the profile of the drop was then extracted in order to determine the surface tension. The results reported in Figure 4 seem to indicate a continously decreasing surface tension as a function of the copolymer concentration. However, this decrease radically differs from the classical surface-active behaviour: no saturation is observed in the surface tension values at highest concentrations, and in that way no critical micellar concentration can be defined. This behaviour is all the more surprising because no surface-active property is expected for this rod-coil copolymer, since neither polystyrene nor poly(*p*-phenylene) is soluble in water. The explanation for this behaviour has been discovered during the surface tension measurements. Indeed, the visualization of the drop allowed us to notice the presence of a solid envelope around the drop. In fact, this solid layer seemed to be formed at the interface of the system during the growing of the drop. Therefore, it was clinged to the interface, which renders difficult its observation. On the other hand, when the solution contained inside the drop was partially sucked up, the solid layer was made clearly visible (see Fig. 4). It was also observed that this envelope was all the more significant as the polymer concentration was increased in the solution. So it appears highly believable that the presence of this solid layer around the drop drastically affected the profile from which the surface tension was determined. Thus, the decrease of the curve observed in Figure 4 is not at all related to the surface-active properties of the copolymer, but clearly indicates that the formation of the envelope is more pronounced as the polymer concentration is increased in the solution. On the other hand, no significant variation of the surface tension was observed in the case of linear PS ($M_w = 10^6$) and in the same time, no polymeric layer surrounding the drop was observed.

3.3 Spreading experiments

A demonstration of the particular wetting properties in this system can be made through spreading experiments. It consists in deposing an amount of solution (1 cm^3) on water and in measuring the area of the resulting lens. The water surface was formed by introducing distilled water into a cylindrical glass cell (diameter $\approx$ 10 cm). The cell was closed by means of a glass cover in order to limit the

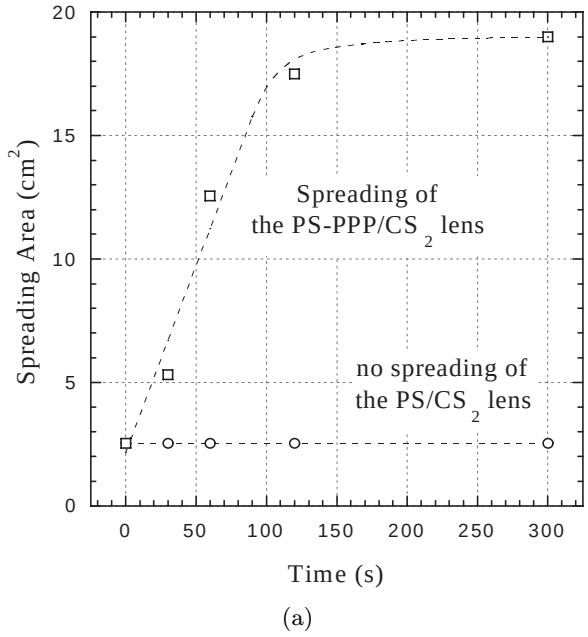

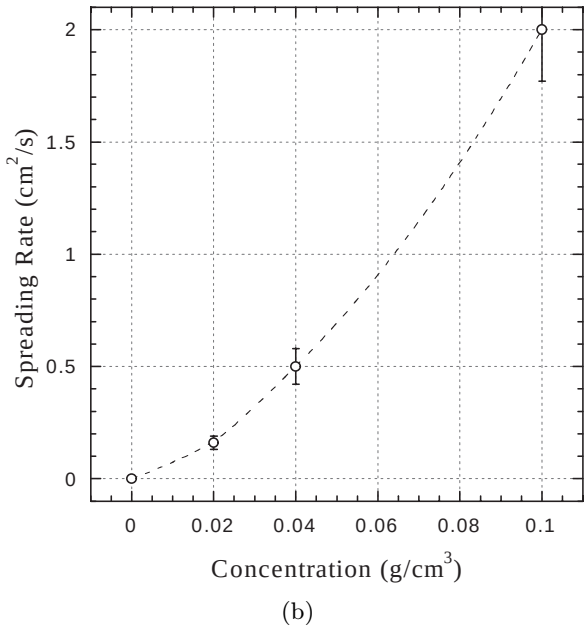

Fig. 5. Spreading of polymer/CS_2 lenses on water. (a) Lens area as a function of time for PS-PPP ($C_0 = 0.02$ g/cm^3; $M_w = 30\,000-3\,000$) and linear PS ($C_0 = 0.02$ g/cm^3; $M_w = 10^6$) in CS_2 solutions. (b) Spreading rate of PS-PPP/CS_2 lenses as a function of the PS-PPP concentration C_0.

evaporation of the floating lens. However, the evaporation was not completely prevented so that the polymer concentration was not constant (this is also the case during the formation of the membrane). The visualization of the water surface by means of a CCD camera allowed the measurement of the spreading area of lenses floating on water as a function of time. Figure 5a shows the spreading area of a solution lens (PS-PPP/CS_2 0.02 g/cm^3) as a function of time. The results for a linear PS ($M_w = 10^6$) at the same concentration are plotted for comparison. While the lens area remained unchanged in the latter case, the initial lens area was increased by a factor 6 for the PS-PPP solution. Besides, the spreading is caracterized by two different regimes: the first one corresponds to a strong increase in the lens area, whereas the second one refers to a slower evolution. Considering the spreading rate, an averaged value can be defined over the duration of the first regime. Spreadings for several solutions with increasing initial concentrations were performed, allowing to plot the averaged spreading rate as a function of the initial concentration (Fig. 5b). The results show that the spreading is faster when the solution concentration increases. Obviously, this phenomenon must be related to the presence of the polymer layer at the interface: the three phases equilibrium is broken when the polymer layer is formed and the contact line is displaced under the action of surface tension forces. It seems highly plausible that this layer results from a polymer precipitation process: in this case, the contact line advancing rate directly depends on the polymer precipitation rate, which is related to the polymer concentration in the solution. As observed in the surface tension measurements, the formation of the polymer layer is all the more significant as the polymer concentration is increased in the solution.

4 Optical microscopy observations

We attempted to observe with a microscope the water vapour condensation process during the formation of the membrane. Four solutions have been studied: PS-PPP/CS_2 (I), PS-PPP/$C_2H_4Cl_2$ (II), PS-PPP/CH_2Cl_2 (III) and PS ($M_w = 10^6$)/CS_2 (IV). The solutions concentration was equal to 0.02 g/cm^3. First experiments have been carried up within optimal conditions for preparing the membranes: $\sim 50\,\mu$l of solution were spread on a glass plate and a flow of water vapour saturated nitrogen was sent toward the liquid surface at room temperature (more details on the preparation method can be found elsewhere [5]). First, we have to notice the unexpected ability of solution II to produce ordered microporous membranes (see Fig. 1). On the other hand, solutions III and IV produced membranes with irregular pore shape and with a broad pore size distribution. Unfortunately, the extreme rapidity by which the structure set up (within ten second under these conditions) rendered impossible the direct observation by optical microscopy. For this reason, a special cell has been designed (see Fig. 6). It is composed of a metallic part in which a cylindrical cavity (diameter ≈ 10 mm, height ≈ 1 mm) has been bored. The bottom of this part was in contact with a Peltier element, allowing the cooling of the solution contained inside the cavity, and the upper face was closed by means of a glass plate. A weak gas flow was allowed to skim over the solution surface. The gas flow was composed of nitrogen saturated with water vapour (the flow of nitrogen bubbled through two flasks of distilled water at room temperature before

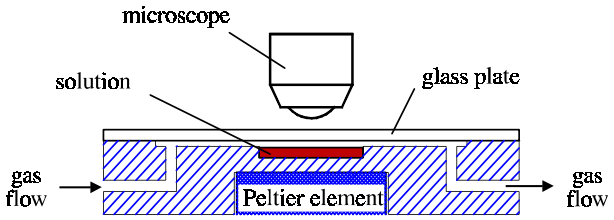

Fig. 6. Schema of the cell used during the visualization experiments. A weak gas flow (water vapour saturated nitrogen) is allowed to skim over the solution surface. The solution is cooled by means of a Peltier element in order to limit the solvent evaporation.

entering the cell). The solutions (I, II, III and IV) were introduced into the cell and their surface was observed during the condensation process. Again, the surface was hardly visible with high magnification because of rapid surface currents due to the solvent evaporation (although the solution was maintained at a temperature close to 5 °C in order to limit the solvent evaporation) and to the gas flow. Nevertheless, floating micron-sized droplets were distinguished at the surface of each solution. Since significant surface currents displaced the droplets over large distances (several times the size of the observed area), only qualitative information about the surface evolution can be subsequently reported. In the case of solutions III and IV, a broad polydispersity was observed in the droplets size, resulting from a large number of coalescence processes. These observations are in good agreement with the morphology found for the membranes prepared from these solutions. On the other hand, solutions I and II have revealed the presence of monodisperse droplets. It was surprising to notice that these droplets came into contact without coalescence, allowing a large variety of patterns to be formed. In fact, they seemed to behave like solid particles (see Fig. 7). Small islands resulting from droplets aggregation were formed and grew by capturing new droplets. We observed well-ordered areas separated from the others either by disordered areas or grain boundaries. Many rearrangements could occur so that well-defined strings of dislocations were formed. At this stage, the floating droplets array looked like a "polycrystal". In these particular preparation conditions, the final structure (*i.e.* large "crystallites" separated by grain boundaries) was rarely observed. Besides, the removal of the gas flow (before the complete evaporation of the solvent) provoked the vanishing of the structure through the water droplets evaporation.

5 Discussion

The sol/gel temperature measurements have revealed that the gelation process was not significantly different between solutions producing well-structured membranes and those producing disordered membranes. Besides, the polystyrene gel phase has never been observed in chlorated solvents [9]: the discovery of $C_2H_4Cl_2$ as a solvent

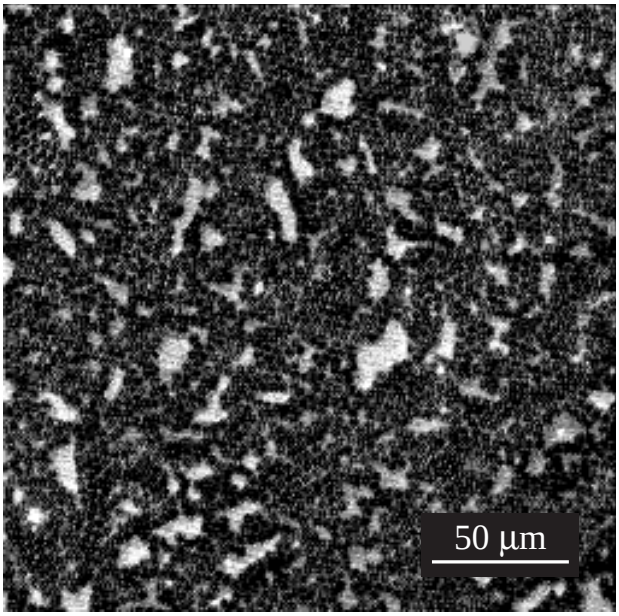

Fig. 7. Photograph of the solution surface during the condensation process. Monodisperse floating water droplets (dark areas) are found to aggregate, forming more or less ordered islands. Visualization of the surface required to reduce the surface currents (by using a weak gas flow and by cooling the solution) though they are essentials to produce ordered compact areas. The membranes obtained in these particular conditions of observation are generally weakly ordered.

giving rise to the ordered structure definitely turns down the assumption made on the importance of the gel phase in this process.

The observation of a water drop floating on CS_2 has revealed a quasi-spherical shape in accordance with the pore shape observed in the membranes. Moreover, it can be deduced from this profile that the curvature of the solution surface, close to the condensed droplets, induces the appearance of an attractive capillary force acting on the droplets. The Bond number $B_o = (\rho_S - \rho_A)gR^2/\gamma_{AS}$ compares the gravity effects to the capillary ones. As $B_o \sim 10^{-7}$ for the condensed droplets, an expression for the capillary force can be given as a function of the separating distance l for $l \ll l_c$ [10,11], where $l_c \sim 1.6$ mm is the capillary length of the solution/air interface:

$$F(l) = -\frac{8\pi R^6 g^2(\rho_s - \rho_A)^2}{9l\gamma_{AS}} \times \left[\frac{\rho_W - \rho_A}{\rho_S - \rho_A} - \frac{1}{2} - \frac{3}{4}\cos\theta + \frac{1}{4}\cos^3\theta\right]^2 \quad (2)$$

where R is the droplets radius; ρ_w, ρ_S and ρ_A are the densities of water, solution and air respectively; γ_{AS} is the solution/air surface tension; $\cos\theta$ is given by expression (1) for the solution/air interface.

The study of the wetting properties in this system has also revealed the presence of a solid layer encapsulating the immersed part of the water droplets. The mechanical resistance of this layer has been tested by forming

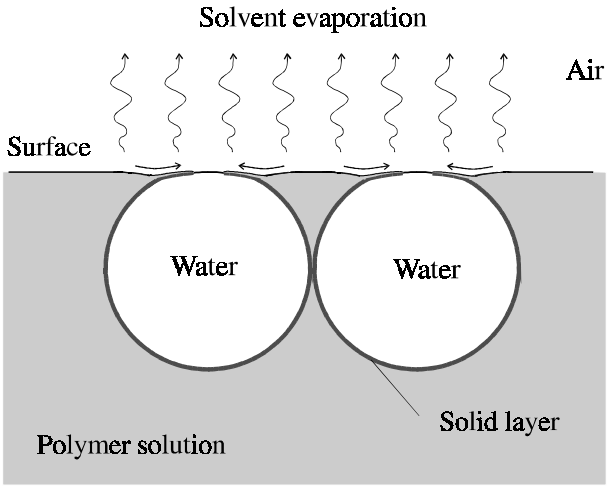

Fig. 8. Schema of the mechanism of formation of the membranes. Water vapour condenses on the solution surface in the shape of micron-sized water droplets. The precipitation of the polymer at the solution/water interface is responsible for the spreading of the solution on the emerged part of droplets and for the formation of a solid layer which completely encapsulates the droplets and prevents their coalescence. Important surface currents and capillary forces contribute to form compact ordered sheets of droplets. After the solvent evaporation, water evaporates in his turn by bursting the polymer layer on the top of droplets, leading to the situation shown in Figure 1.

two millimetric solution drops in water and by pressing one against the other. It was observed in the case of PS-PPP/CS_2 solutions that the polymer layer was sufficiently resistant for preventing the coalescence, even when the radius of the contact area was close to the drop radius. On the other hand, drops of linear PS ($M_w = 10^6$)/CS_2 solution coalesced when pressed together. We think that the formation of the layer results from the precipitation of the polymer, and this seems to be confirmed by X-rays scattering experiments: while the characteristic length between the PPP cores of the micellar aggregates has been found to be about 209 Å in the case of featureless membranes (prepared in dried atmosphere), a smaller one (139 Å) has been measured in the structured membranes (prepared in the presence of moisture) [12]. The reduction of the characteristic length in the case of ordered membranes can be related to a "precipitated-like" state for the polymer. One other interesting consequence of the polymer precipitation is the ability of the solutions to spread on water. While CS_2 do not spread on water surface (the spreading coefficient in the case is approximately -2 erg/cm^2), PS-PPP/CS_2 solutions spread at a rate proportional to the polymer concentration. As a consequence, the solution is allowed to spread on the emerged part of the water droplets, as shown in Figure 8. A thin polymer film is thus formed on the top of the droplets, probably stopping their growing. We expect that the kinetic of formation of this film may play an important role in the droplet size regulation. Besides, the presence of this film on the top of each droplet has been proved: as the best part of the solvent is evaporated, the membrane temperature rises up the ambient temperature and water contained inside the droplets evaporates by bursting the polymer film, leading to the formation of the circular holes network observed on the membranes surface. In some cases, the layer is not bursted because connections are formed between neighbouring pores.

We argue that polymer precipitation is a key parameter in the mechanism of formation of ordered membranes as it allows the droplets to behave like "solid" particles trapped at the solution surface. Previous experiments have shown that water droplets condensed on an oil surface could produce regular patterns ("breath figures"). In that case, coalescence was delayed (but not prevented) because droplets in contact had first to eliminate the separating oil film [13,14]. In the same way, aggregation processes have been observed in the celebrated "bubble raft" experiments of Bragg and Nye [15]. Soap bubbles ($R \sim 1$ mm) constituting this system crystallize under the influence of capillary attractive forces as closed-packed hexagonal sheets. The presence of surface-active molecules at the air/solution interface prevented coalescence for a few hours. In our case, the polymer layer encapsulating the droplets highly prevents the coalescence. In that way, a repulsive term resulting from the internal pressure of the droplets arises as they touch. This attractive-repulsive potential seems to be an important element in the establishment of the structure, since it allows to locally arrange the droplets in a stable compact hexagonal geometry. Note that the absence of polymer precipitation in the case of the linear PS/CS_2 or PS-PPP/CH_2Cl_2 tested solutions has been found to be the drastic reason for the droplets coalescence and for the formation of disordered membranes. The presence of capillary interactions is not sufficient to obtain compact sheets. In fact the calculation of the capillary energy (assuming capillary forces given by expression (2)) shows that the bonding energies are several orders of magnitude smaller than the thermal energy k_BT. Moreover, surface currents (due to the gas flow, convection and Marangoni flows) observed during the optical microscopy experiments induced large shear effects at the solution surface. As water droplets rapidly fill the whole solution surface, Brownian motion and shear effects contribute to organize the floating "raft" as packed sheets. As the condensation process goes on until the solvent be entirely evaporated, new droplets may grow on the sites of the triangular network constituted by the first floating layer. In that way three-dimensional structures are sometimes formed though the lower layers are usually discontinuous and not always well-ordered.

We have to notice that the formation of ordered two-dimensional aggregates has previously been observed in similar conditions. In his classical work on determining the Avogadro number, Perrin [16] used a suspension containing monodisperse spherical particles of gomme-gutte. Some amount of this suspension was deposited on a glass plate and dried slowly. More recently, two-dimensional arrays of latex particles have been obtained by removing the volatile solvent from a thin layer of suspension. In

this latter case, the formation of the ordered structure is achieved in the last stages of the evaporation process, due to the presence of "immersion" capillary forces arising in the system when the thickness of the layer is smaller than the particle diameter [17]. However, this mechanism is not relevant in our system since microscopy observations have shown that the structure established in the earlier stages of the mechanism. Moreover, the high viscosity resulting from the solvent evaporation will not allow rearrangement processes when the solution thickness is of the order of the droplets diameter.

An interesting question remains about the ability of the star-polystyrenes to produce structured membranes while disordered membranes are obtained from usual linear polystyrenes. We believe that this specific behaviour is exclusively related to the capacity of the former to precipitate at the interface of the system. In that sense, the star-polymer microstructure seems to be a determinant element for producing well-ordered structures. For example, synthetized block copolymer polystyrene–poly-3-hexylthiophene (PS-P3HT) [18] with conjugated sequence soluble in CS_2, does not lead to any special morphology in its undoped state. But after a light doping of the P3HT sequence by $FeCl_3$ the regular morphology is observed. Neutron scattering experiments have shown that the electrically charged P3HT sequences associate with star-like micelles formation [19].

6 Conclusions

The results presented in this paper permit to draw the main outlines of the mechanism of formation of ordered micro-porous polymeric membranes: first, evaporation of the solvent induces the cooling of the solution surface and the surrounding water vapour is condensed in the shape of floating spherical droplets (see Fig. 8). The formation of compact hexagonal sheets is promoted by important surface currents and by the presence of an attractive-repulsive interaction potential between droplets, which locally arrange them in a stable compact hexagonal geometry. In these compact aggregates, coalescence is prevented by the formation of a solid polymer envelope encapsulating each droplet. It has been shown that the key parameter in the establishment of the morphology is the capacity of the polymer to precipitate at the solution/water interface. Contrary to PS-PPP and star-PS, usual PS has not been found to precipitate at the solution/water interface. This seems to be the main reason why usual PS/CS_2 tested solutions do not produce well-ordered membranes. Another solvent ($C_2H_4Cl_2$) has been found to give similar results to CS_2, which proves that the gelation process is not a determinant element in this process. This discovery relaunches the hope of finding other systems "polymer/solvent/non-solvent" allowing to produce regular structures provided that the particular wetting properties be satisfied. Nevertheless, a lot of work remains to be done in the control of the pore size. In particular, a systematic study of the influence of the preparation parameters has to be performed.

References

1. G. Widawski, M. Rawiso, B. François, Nature **369**, 397 (1994).
2. M. Möller, E. Müleiser, J. Omeis, *Physical Networks Polymers and Gels*, edited by W. Buchard, S.B. Ross-Murphy (Elsevier, Amsterdam, 1988).
3. G. Widawski, M. Rawiso, B. François, J. Chim. Phys. **89**, 1331 (1992).
4. N. Lehsaini, N. Boudenne, J.G. Zilliox, D. Sarrazin, Macromol. **27**, 4353 (1996).
5. B. François, O. Pitois, J. François, Adv. Mater. **7**, 1041 (1995).
6. A. Takahashi, M. Sakai, T. Koto, Polym. J. **12**, 335 (1980).
7. H.M. Princen, *Surface and Colloid Science*, edited by E. Matijevic (Wiley-Interscience, 1969), Vol. 2.
8. A.W. Adamson, *Physical chemistry of surfaces*, 3rd ed. (Wiley-Interscience, 1976), p. 26.
9. H.M. Tan, Hilner, Baer, Macromol. **16**, 28 (1983).
10. M.M. Nicolson, Proc. Cambridge Philos. Soc. **45**, 288 (1949).
11. D.Y.C. Chan, J.D. Henry, L.R. White, J. Colloid Interface Sci. **79**, 410 (1981).
12. G. Widawski, thesis, University of Strasbourg, France, 1993.
13. R. Merigoux, C. R. Acad. Sci. (Paris) **207**, 47 (1938).
14. A. Steyer, P. Guenoun, D. Beysens, Phys. Rev. E **48**, 428 (1993).
15. W.L. Bragg, J.F. Nye, Proc. Roy. Soc. A **190**, 474 (1947).
16. J. Perrin, Ann. Chim. Phys. **18**, 1 (1909).
17. K. Nagayama, Phase Transitions **45**, 185 (1993).
18. B. François, G. Widawski, M. Raviso, B. César, Synth. Met. **69**, 463 (1995).
19. B. César, M. Raviso, B. François, unpublished.